Inter-step-edge correlations on crystalline surfaces measured with helium-atom scattering

B. J. Hinch* and J. P. Toennies
Max-Planck-Institut für Strömungsforschung, Bunsenstrasse 10, Postfach 2853, D-3400 Göttingen, Federal Republic of Germany
(Received 11 August 1989; revised manuscript received 16 February 1990)

For close-packed metal surfaces the large-angle scattering of helium atoms is dominated by short-range interactions with surface defects. Along certain azimuths, monatomic step edges are the major contributors to diffuse scattering. The broad intensity oscillations provide information on the local step shape, and the finer structure is an indication of interstep correlation, which becomes more prevalent at higher step densities. Differently oriented step edges scatter along different final azimuths and thus the correlations between like step edges are only observed. The energy dependence of angular scans has been used to investigate the correlation between step edges on a sputtered Cu(111) surface. Comparison with structure-factor calculations indicates the presence of (331) and (211) microfacets.

I. INTRODUCTION

The appearance of step edges on a crystalline surface is an indication of the onset of disorder or even of roughening of a surface. On entropy grounds, a surface cannot be prepared without steps. Many surface studies have been performed assuming that the step density is sufficiently low that the results are unaffected, but, increasingly, the influence of steps is known to be of importance in many physical processes. Step edges are known to play a dominant role in determining the limited correlation lengths in phase transitions,[1] increased sticking coefficients,[2] increased reactivity of adsorbates,[3,4] preferred orientations of superlattices, or simply the presence of surface facets.

Electron diffraction has a certain surface sensitivity, and has been used successfully in the characterization of step densities and distributions.[5] This information is deduced, perhaps somewhat indirectly, from the scattering from terraces (unstepped regions). When the correlation over the surface is broken up, it is assumed that, on a single-crystal face, this results from the presence of a step edge. With careful studies, over many kinematic scattering conditions, it is also possible to deduce the distribution of step heights.[5,6]

In contrast to all other diffraction-scattering probes, however, atoms and molecules are the only ones which interact directly with step edges. The long-range interaction of atom-surface scattering, contrary to all point-scattering methods, implies that a step edge has a finite scattering cross section. This was first observed experimentally for specular helium-atom scattering (HAS) from a randomly stepped Pt(111) surface.[7] At a kinematic (Bragg) condition such that all terraces scatter in phase, the decrease of intensity of the specular peak with increasing step density was assigned to a step-edge cross section, ~ 10 Å^2 per unit length. The majority of this intensity is scattered through only small angles. The same system was later observed to show characteristic intensity oscillations in the large-angle scattering along $\langle 11\bar{2}\rangle$-type azimuths.[8] It has been demonstrated that these oscillations contain information on the short-range interactions of He with extended surface steps.[9–11] More recently, similar measurements from many surfaces have been reported.[12,13] In most of these experiments additional sharp "fine-structure" features have been identified in the large-angle diffraction. Originally it was thought that this fine structure might arise from the diffraction from isolated step edges.[10] Since then it has become apparent that the observed fine structure is, in fact, dependent on surface preparation and treatments.[12] Thus the independently suggested explanation that the variable fine structure arises from interstep correlation effects[14] (lattice-gas effect) now seems more likely to be correct.

If a significant proportion of steps are separated by distances which are shorter than an experimental transfer width at the surface,[15] then an interference from several steps (step-step correlation) will be observable. For HAS the transfer width depends on the incidence angle and energy and is typically of the order 100–200 Å. The effects are therefore most prevalent with higher step-edge densities. If the fine structure is observed, it provides much information on interstep correlation on the target surface. This paper investigates both experimentally and computationally the type of information available from the fine structure in large-angle diffuse-scattering measurements, and makes explicit conclusions about the topology of a Cu(111) surface after one particular ion-bombardment treatment. The methods illustrated here could clearly be extended to any close-packed smooth surface under almost any degree of disorder or roughness.

II. EXPERIMENT

The copper crystal was cut to within 0.25° of the (111) face, mechanically polished to a grade of 1 μm, and placed in vacuum. The surface was cleaned by repeated cycles of $\frac{1}{2}$-h, 1-kV-Ne$^+$ (2.0 μA cm^{-1}) sputtering and flashing to 800 K. The contaminant levels, as measured

with a cylindrical mirror analyzer (CMA), were estimated from 3-kV-electron-induced Auger spectroscopy to be sulfur [S]$<0.2\%$, [C]$<0.5\%$, and [O]$<0.5\%$. High-temperature flashes to greater than 900 K induced further segregation of sulfur to less than 2%. This situation was, however, easily avoided during the measurements presented here, as a very-high-quality, well-annealed surface was not required in these experiments.

The measurements were made in a HAS apparatus, which is fully described elsewhere.[16] Only the basic features of its design are discussed here. A supersonic expansion He-atom source produces an intense atomic beam with a velocity resolution $\Delta v/v \cong 1\%$. This beam is scattered from the crystal, and intensity is measured at the detector, which, in these experiments, is placed at an angle of 90° from the incident direction. The angles of incidence, θ_i, and of emergence, θ_f, are varied simultaneously by rotating the crystal through an axis perpendicular to the scattering plane. For in-plane scattering this implies the fixed-geometry condition, $\theta_i+\theta_f=90°$. A typical angular scan, $0°<\theta_i<90°$, in 0.2° steps, takes on the order of 12 min. The sample chamber has a base pressure of less than 7×10^{-11} mbar and the surface was not observed to contaminate during the course of these measurements.

The He-atom–source temperature was varied between 110 and 330 K, producing beams of energies 24.5–75 meV. The exact beam energies were calibrated using time-of-flight (TOF) measurements at each source temperature.

The diffraction at large angles far from specular was investigated along the $\langle 11\bar{2}\rangle$ azimuth. The quality of the crystalline surface was degraded by ion bombardment at controlled surface temperatures, producing many monatomic steps.[12] These were observed from their characteristic diffuse-intensity oscillations. Multiple step-height step edges were not observed in the measurements presented here, but may well be present in small concentrations.[17] Not only quantitative but also qualitative changes in the diffuse-intensity oscillations were observed after anneal treatments. These have been investigated at different step densities and also at varying incident wave vectors.

III. RESULTS

The two upper intensity curves of Fig. 1 were taken under identical incident-He-atom-beam conditions, but with different surface preparations. Curve (a) shows a typical angular scan taken at 225 K after sputtering at 275 K for 1 h (0.7 μA cm^{-2}, Ne^+, 1 keV) and standing a further hour at 225 K. Curve (b), in contrast, is taken (at 225 K) almost immediately after a similar sputter treatment, but at 300 K. The total diffuse (nonspecular) scattered intensity is reduced, reflecting a smaller density of step edges. From a one-dimensional (1D) model, linear step densities of order $\frac{1}{25}$ and $\frac{1}{75}$ Å^{-1}, respectively, would be estimated.[10] Curve (b) shows the typical intensity oscillations expected from a low density of uncorrelated, or isolated, step edges on the fcc (111) face. This type of intensity oscillation was first measured from a Pt(111) surface[8] and has since been observed for other step edges on Al(111) and Ni(001).[12,13] In the limit of low step density the diffuse intensity is expected to be simply proportional to the absolute step density, but, at higher densities, as observed here, other structure develops. This was even evi-

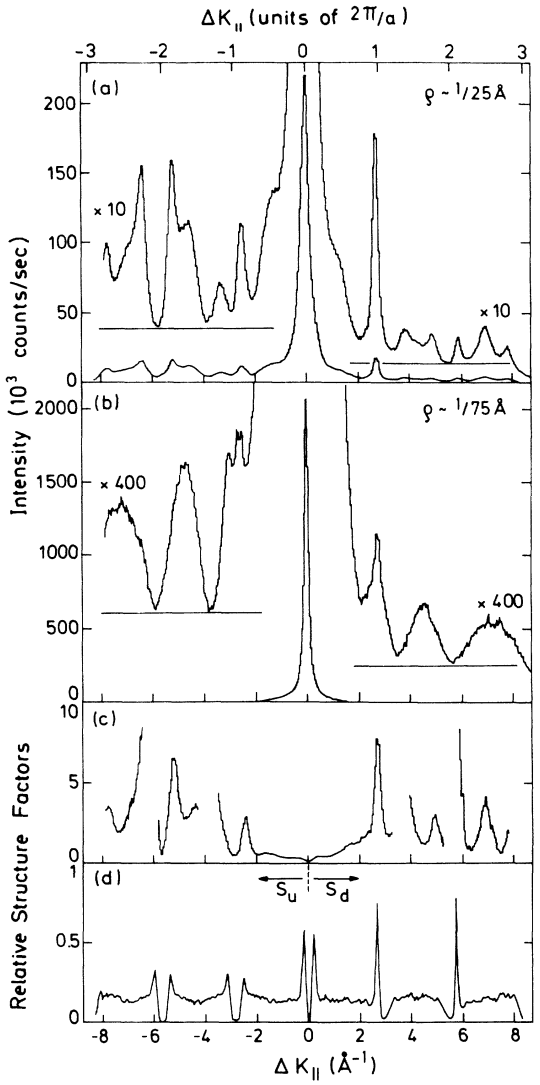

FIG. 1. Measured intensities and calculated structure factors for the Cu(111) surface along the $\langle 11\bar{2}\rangle$ azimuth. Curve (a), measured after sputtering a well-annealed surface for 1 h at 275 K with 1-keV-Ne-ion current of 0.7 μA cm^{-2}. Curve (b), after a similar treatment at 300 K; see text. Both curves measured with surface temperature $T_{Cu}=225$ K and incident wave vector $k_i=9.1$ Å^{-1}. Horizontal lines indicate uniform local background levels (a) 3.85 and 1.40 kHz and (b) 1.50 and 0.63 kHz used for background subtraction in the generation of curve (c). (c) Estimate of relative structure factors, S_u (lhs) and S_d (rhs), for the distribution of steps observed in curve (a). Note that these curves are very sensitive to background subtraction. See discussion in text. (d) Calculated structure factors, for the angular scans above, using the step-distribution model discussed in the text. $k_i=9.1$ Å^{-1}, $\bar{t}=3a$, $\sigma_t=3a$, $U=D=1000$, $L=7841a$, and $p_{ch}=0.15$.

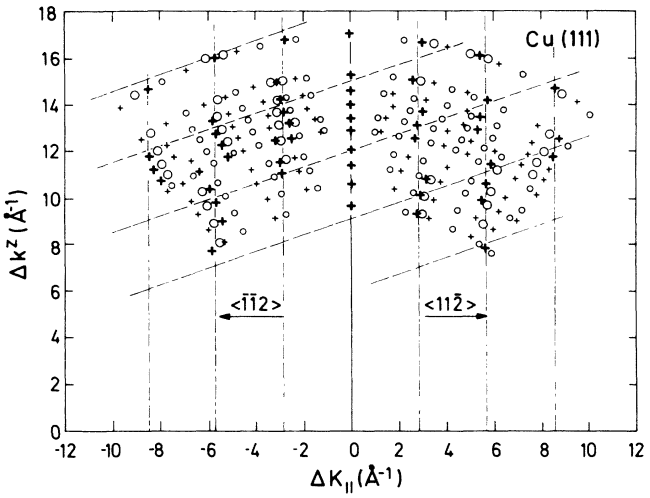

FIG. 2. Maxima (+ symbols) and minima (circles) in angular scans, at varying incident energies, plotted in momentum-exchange space. The measurements, at $T_{Cu}=225$ K, follow a sputter treatment of 1 h (0.7 μA cm^{-1}) of Ne^+ at $T_{Cu}=300$ K. Active features have been identified and designated by larger symbols. Positive parallel momentum transfers ($\Delta K_{\|}$) correspond to transfers along the scattering azimuth, the $\langle 112 \rangle$ direction. Vertical dashed lines indicate the 2D Bragg conditions, $\Delta K_{\|}=2n\pi/a$. Other dashed lines are of the form $\Delta k^z h=\Delta K_{\|} a/3+2n\pi$. The points of intersection of dashed lines are the 3D Bragg conditions.

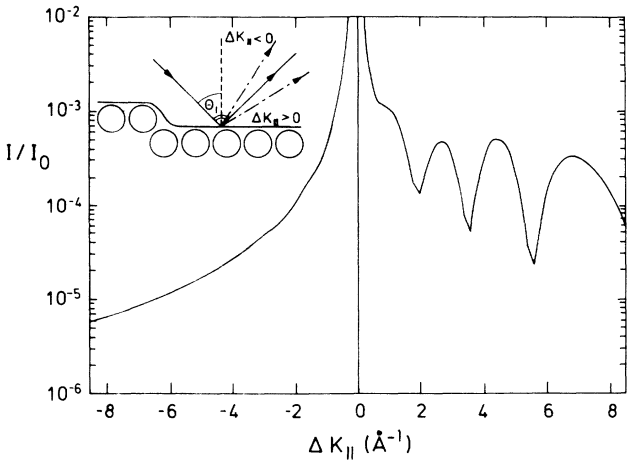

FIG. 3. Normalized intensities calculated for a density of $\frac{1}{150}$ Å of downhill steps at incident wave vector, $k_i=9.1$ Å^{-1}. Note that the largest proportion of scattered intensity, other than that associated with specular intensity, is found in positive parallel momentum exchange only. Calculational parameters (Ref. 10) are step height $h=2.09$ Å, width $W=5.3$ Å, steepest angle of descent, $\varepsilon=43°$, and reciprocal correlation length, $\gamma=0.02$ Å^{-1}. Inset shows geometry for step-down scattering.

dent on the fairly low-step-density Pt(111) surface.[8] It is now clear that the so-called "fine structure" is not only dependent on the absolute step density, but also on the exact means of surface preparation. This leads to the interpretation in terms of interstep correlations.[14] The diffuse intensity is no longer simply proportional to the step-edge density, but now depends on more subtle features of terrace shapes, sizes, and step-edge interactions. A discussion of the models used in deriving the curves of Figs. 1(c) and 1(d) will follow later.

Comparing Figs. 1(a) and 1(b), it is possible to identify "active" features in the angular scan. Both sharp maxima and sharp minima are observed as a result of increasing step density. We refer to these *new* maxima and minima as the active features of an angular scan at any particular incident energy. Similar measurements were made over a range of incident energies, for the surface after 1 h of sputtering at 300 K. Active features were identified throughout, and their positions in reciprocal space have been plotted in Fig. 2. This demonstrates the positions of all possible maxima (+ symbols) and minima (circles) observed in scattering space. The special active features have then been marked with the enlarged symbols. The pattern of active features is clearly asymmetric with respect to the $\Delta K_{\|}=0$ line. The diffraction from a stepped fcc (111) surface no longer shows sixfold symmetry, but rather threefold symmetry. The origin and **k**-space dependence of these active features are the subject of the next section.

IV. INTERPRETATION AND DISCUSSION

The kinematics of diffuse HAS from a stepped fcc (111) surface is much simpler than the equivalent theory for low-energy electron-diffraction (LEED) scattering for the following reasons.

(1) The terraces of fcc close-packed (111) surfaces show no significant corrugation to helium atoms. This approximation implies that terraces scatter He atoms only into directions close to specular.

(2) The large-angle scattering along $\langle \bar{1}\bar{1}2 \rangle$- and $\langle 11\bar{2} \rangle$-type azimuths arises from the extended step-edge potential and is dominated by the short-range repulsive interactions. Hard-wall models reproduce this type of scattering well. Analogous diffuse scattering from LEED experiments can only arise from the absence of multiple-scattering mechanisms at atomic cores close to step edges.

(3) HAS from downhill steps lead almost exclusively to transfer into states of positive parallel momentum exchange, $\Delta K_{\|}$. In contrast, uphill steps (risers) scatter into negative $\Delta K_{\|}$ only. Such asymmetries in the form factors are not expected for electron diffraction.

Figure 3 illustrates the latter point. The calculated intensities from an isolated-model hard-wall downhill step (see inset) produces the characteristic step-edge oscillations on one side of specular only. This has not been explicitly tested experimentally, as most surfaces have equal numbers of uphill and downhill steps. Vicinal surfaces, having an unequal balance of step directions, usually have relatively strong step-step correlations. However, these surfaces[18,19] do exhibit strong symmetries in intensity with respect to the terrace specular direction.

A general one-dimensional kinematic theory of scattering predicts a scattered amplitude $A(\Delta \mathbf{k})$ given by

$$A(\Delta\mathbf{k})=\frac{1}{L}\left[\sum_{l=1}^{T}F_{t,l}(\Delta\mathbf{k})e^{i\Delta\mathbf{k}\cdot\mathbf{r}_l}+\sum_{m=1}^{U}F_u(\Delta\mathbf{k})e^{i\Delta\mathbf{k}\cdot\mathbf{r}_m}+\sum_{n=1}^{D}F_d(\Delta\mathbf{k})e^{i\Delta\mathbf{k}\cdot\mathbf{r}_n}\right]. \quad (1)$$

The total momentum transfer $\Delta\mathbf{k}$ is composed of the two x and z momentum-transfer components, $\Delta\mathbf{k}=\Delta K_{\parallel}\hat{\mathbf{x}}+\Delta k^z\hat{\mathbf{z}}$. $F_{t,l}$ is the terrace form factor of the lth terrace from a total of T terraces. L represents the total length of a unit cell used to model a stepped surface of any given step-edge distribution. F_u and F_d are the form factors for scattering from step edges of up and down orientations, respectively. For a unit cell that conserves the macroscopic plane, the total number of downhill steps, D, equals the number of uphill steps, U, and is $T/2$. $\mathbf{r}_l$, $\mathbf{r}_m$, and $\mathbf{r}_n$ represent the coordinate vectors of the lth terrace, mth uphill step, or nth downhill step, respectively.

As mentioned before, for HAS this can be considerably simplified. For "larger" positive $\Delta K_{\parallel}$ we have $F_u\sim 0$ and $F_{t,l}\sim 0$. Thus Eq. (1) reduces to

$$A(\Delta K_{\parallel}>0,\ \Delta k^z)=\frac{1}{L}\sum_{n=1}^{D}F_d(\Delta k)e^{i\Delta\mathbf{k}\cdot\mathbf{r}_n}. \quad (2)$$

Likewise, for negative $\Delta K_{\parallel}$, not close to $\Delta K_{\parallel}=0$,

$$A(\Delta K_{\parallel}<0,\ \Delta k^z)=\frac{1}{L}\sum_{m=1}^{U}F_u(\Delta k)e^{i\Delta\mathbf{k}\cdot\mathbf{r}_m}. \quad (3)$$

The diffuse intensities are then given by

$$I(\Delta K_{\parallel}>0,\ \Delta k^z)=\frac{D^2}{L^2}|F_d|^2\langle e^{i\Delta\mathbf{k}\cdot(\mathbf{r}_n-\mathbf{r}_n')}\rangle \quad (4a)$$

$$=\frac{D^2}{L^2}|F_d|^2S_d(\Delta\mathbf{k}) \quad (4b)$$

and

$$I(\Delta K_{\parallel}<0,\ \Delta k^z)=\frac{U^2}{L^2}|F_u|^2\langle e^{i\Delta\mathbf{k}\cdot(\mathbf{r}_m-\mathbf{r}_m')}\rangle \quad (5a)$$

$$=\frac{U^2}{L^2}|F_u|^2S_u(\Delta\mathbf{k}), \quad (5b)$$

where the angular brackets ($\langle\ \rangle$) refer to a statistical average over all possible pairs of r and r'. The term S_d is the structure factor for all downhill steps. A similar expression, of course, holds for S_u and uphill step edges.

Figure 1 shows how we may estimate a value for the structure factors. Figures 1(a) and 1(b) illustrate the intensities observed under identical scattering conditions. The step density for the second case is considerably reduced. Under these conditions interstep correlations could be assumed to be unimportant. In this case the structure factor is uniform, $S_u=1/U$ and is not dependent on $\Delta\mathbf{k}$. The validity of this assumption is clearly limited, as fine structure is indeed still apparent (at $\Delta K_{\parallel}\sim\pm 2.8$ Å^{-1}), even at the low step density of Fig. 1(b). The curve of Fig. 1(c) is produced after the subtraction of local background levels, indicated in (a) and (b), and the division of curve (a) by curve (b). Curve (c) thus represents a crude estimate of the structure factors for the upper curve (a). The divided curve is not shown for regions of smallest intensities, as the noise levels become very large, and the local background subtraction becomes critical. Curve (d) is to be discussed later. Within the limit of our resolution, the peak positions in the structure factors are identical to those of the sharp diffraction features in the data, Fig. 1(a). The "active" peak positions, as shown in reciprocal space in Fig. 2, therefore coincide with peaks in the structure factor for either uphill steps [left-hand side (lhs)] or downhill steps [right-hand side (rhs)].

To assist identification of 3D Bragg points, dashed lines are drawn in Fig. 2. The intersections of these lines

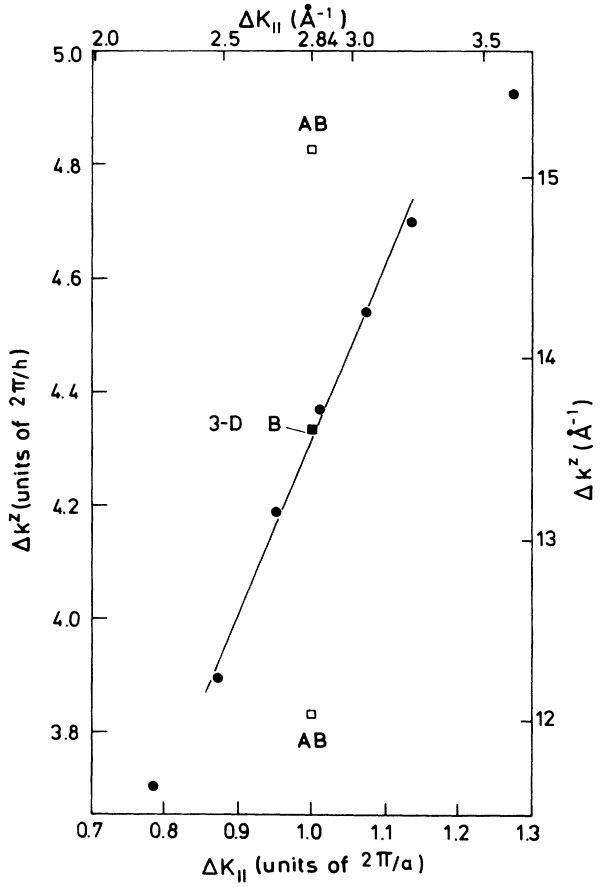

FIG. 4. A small section from Fig. 2 is shown. Circles denote experimental active-feature maxima positions: The solid square represents a 3D Bragg-scattering condition in reciprocal space; the open squares two anti-Bragg conditions (LEED notation).

correspond to the 3D Bragg conditions. It appears that all peaks in the structure factors, which are where we identify active peak positions, lie along lines which run through these 3D Bragg conditions. Step edges are necessarily restricted to the projection of a 3D lattice gas onto the scattering plane. This correlation ensures that scattered phases are identical for all steps (of the same orientation) at the 3D Bragg conditions, $\Delta\mathbf{k}=\Delta\mathbf{k}_{3D}$. This basic argument and observation of larger peak intensities at $\Delta\mathbf{k}_{3D}$ conditions has enabled the identification of the two $\langle\bar{1}\,\bar{1}\,2\rangle$ and $\langle 11\bar{2}\rangle$ directions.[12] Helium scattering is a purely surface-sensitive technique, and without step edges the diffraction from this fcc (111) face is sixfold symmetric. The *ABC*-type stacking of this surface only becomes apparent when sublayers are exposed, or step edges exist, and only then can the threefold symmetry or orientation of the crystal be identified.

Figure 4 demonstrates that peak maxima in the neighborhood of an example 3D Bragg condition lie approximately on a straight line in reciprocal space. This is true of all the active-feature maxima. A gradient in reciprocal space of $3.1a/h$ is observed in this example, where a is the spacing between rows on the (111) surface and h is the step height. For Cu(111), $a=2.21$ Å and $h=2.09$ Å. In reproducing the structure factors, the gradient proves to be a key parameter. From the complete data set presented here, our best estimates of the gradients are 2.5 ± 0.5 for step-up scattering into negative-$\Delta K_{\parallel}$ directions and 2.8 ± 0.4 for positive $\Delta K_{\parallel}$. The relatively large variations in these numbers will, we believe, be resolved when the kinematic model can include a potential-well structure, which could be of extreme significance for the largest angle scattering and for the lowest incident energies.

The following section discusses the properties of the structure factors for differing statistical distributions of step edges. In a manner similar to Ref. 14, a randomly distributed set of step edges is modeled within a large unit cell containing monatomic step edges. An adequate sampling of the step-edge correlations is expected to be simulated within a sufficiently large unit cell. Here, the step-edge directions are defined by one probability distribution and their separations by another. The terrace lengths t are defined by a Gaussian distribution,

$$P(t)=P_0\exp\left[\frac{-(t-\bar{t})^2}{2\sigma_t^2}\right], \tag{6}$$

for $t\geq 1$, where $\bar{t}$ is some mean terrace length and σ_t the standard deviation in lengths. To each terrace length a distance of a third of a lattice-row spacing, $a/3$, is added for steps down, or $2a/3$ for steps up. This construction is illustrated in Fig. 5. For convenience, step-edge positions are then defined as being at the bottom of downhill steps and at the top of uphill steps. The first step is of a defined orientation (up). The remainder of the surface unit cell is then generated by defining a probability for a change in step-edge orientation, at each terrace edge, P_{ch}. In generation of a finite-sized unit cell with periodic boundary conditions, the case of $P_{ch}=0$ cannot be allowed. If $P_{ch}=1$, a structure with only two layers is generated. In the limit of $P_{ch}\rightarrow 0$ the surface consists of large facets, and at $P_{ch}=0.5$ the steps are purely randomly oriented. The structure factors are then calculated using

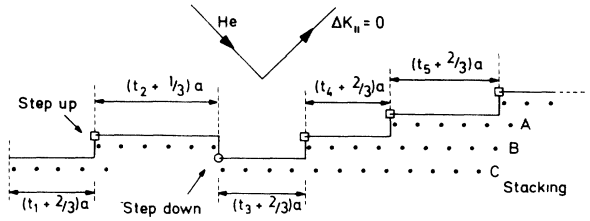

FIG. 5. Schematic section ($\langle 112\rangle$) of a model step-edge distribution. Squares represent the set of step-up coordinates, $\{r_m\}$, and circles that of step-down coordinates, $\{r_n\}$. Dots indicate atom-core positions projected onto the plane of the diagram. The *ABC* stacking of a fcc (111) surface is indicated, illustrating the lack of mirror symmetry in the $[1\bar{1}0]$-type directions.

$$S_u=\frac{1}{U^2}\left|\sum_{m=1}^{U}e^{i\Delta\mathbf{k}\cdot\mathbf{r}_m}\right|^2 \tag{7a}$$

and

$$S_d=\frac{1}{D^2}\left|\sum_{n=1}^{D}e^{i\Delta\mathbf{k}\cdot\mathbf{r}_n}\right|^2 . \tag{7b}$$

Figure 6 shows the results of structure factors from three surfaces. Each has $\bar{t}=3a=6.65$ Å, $\sigma_t=3a$, $U=D=1000$, and $L=7841a$. Three types of surfaces are used: (a) $P_{ch}=0.15$, (b) $P_{ch}=0.5$, and (c) $P_{ch}=0.85$.

The results have been calculated and, for clarity of presentation, are smoothed by the convolution with a triangular function of full width half maximum (FWHM) of $0.02(2\pi/a)$. The smoothing is used to simulate approximately the finite resolution of an apparatus, and to eliminate any artifacts from the modeling of a random distribution with a finite-sized unit cell.

The results of the calculations can be used to rule out case (c), the locally two-level structure with high P_{ch}. The central peak predicted at $\Delta K_{\parallel}\approx 2\pi/a$ independent of Δk^z, which corresponds to a doubled periodicity of the pure two-level system,[20] is not observed experimentally. Case (b), corresponding to random step direction, is shown to illustrate some intermediate-type dispersion of the peak positions. The other extreme of case (a) shows the almost straight-line dispersion that would be expected from the incoherent superposition of intensities from microfacets.

Upon comparison with the computational results of Fig. 7, the results of Fig. 4 clearly indicate a surface describable by a step direction-change probability P_{ch} much smaller than 0.5. This implies the presence of mi-

crofacets on the surface, after the particular surface preparation described above. The model described above, with $P_{ch}=0.15$, was also used in the generation of structure factors illustrated in Fig. 1(c). Microfacets reproduce the structure factors of the higher-step-density surface well. Variation of calculational parameters would produce better fits. A more detailed experimental study of peak positions, which is not yet available, would yield more accurate values of P_{ch}, $\bar{t}$, and σ_t. The data set presented in Fig. 2 took of the order of 4 h (12 min/scan with k_i stabilizations). A more instantaneous set of data should be taken over smaller angular ranges and not necessarily over the full range of possible incident energies. Even at sample temperatures of $T_{Cu}\sim 225$ K the surface anneals out slowly, continually changing the exact form of interstep correlations. For this reason a more accurate evaluation of the data presented here was not considered profitable. However, it can be deduced immediately that the microfacets are of every high step densities. $\bar{t}=3a$ resulted in a gradient of Fig. 7 of order

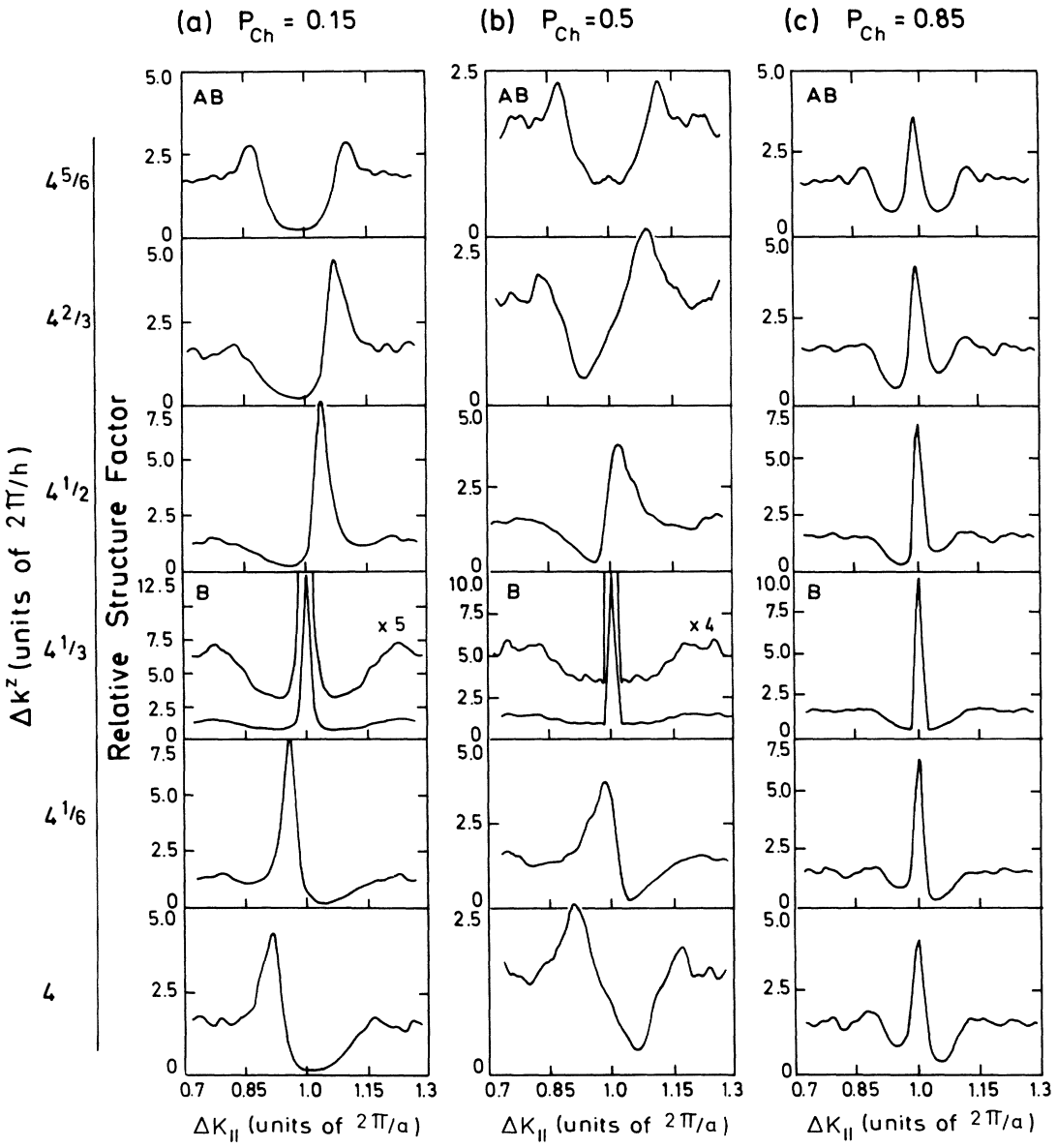

FIG. 6. Calculated structure factors for downhill steps, S_d, as calculated for the statistical step-edge model described in the text. The structure factor S_d is evaluated at constant values of perpendicular momentum transfer, indicated on the left-hand side. The upper curves (AB) run through an anti-Bragg condition. Likewise, the fourth row (B) runs through the 3D Bragg condition. The results from three-step direction-change probabilities—(a) $P_{ch}=0.15$, (b) $P_{ch}=0.5$, and (c) $P_{ch}=0.85$—are illustrated.

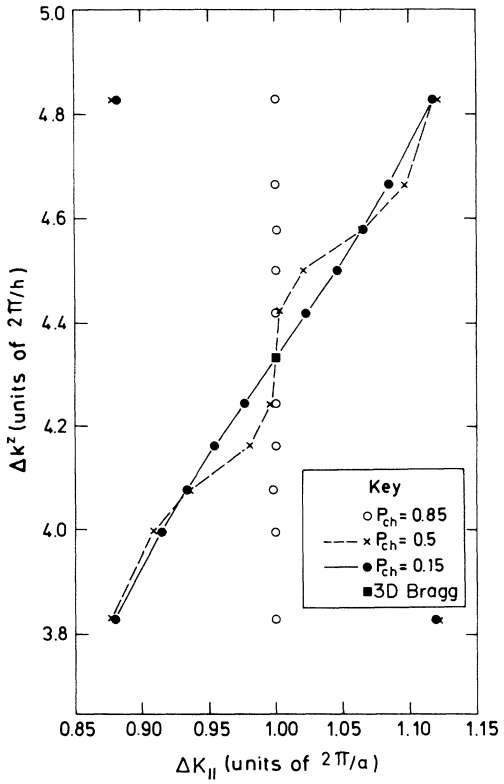

FIG. 7. Structure factor, S_d, maxima positions in reciprocal space for the three statistical step-edge models of Fig. 5. Each model shows a peak at the 3D Bragg condition (square). Lines, drawn to guide the eye, run between calculated points for two models, $P_{ch}=0.5$ and 0.15. The third model, with $P_{ch}=0.85$, always shows a central peak that is almost indistinguishable from that at $\Delta K_{\parallel}=2\pi/a$.

$4.2a/h$. To obtain a gradient comparable with that of the experimental data of Fig. 4, we must assume that most of the facets will have $\bar{t}\sim 2a$, implying, for downhill steps and with this scattering orientation, the presence of many (331) microfacets. Similar considerations of scattering from uphill steps also imply many (211) microfacets. Clearly, the whole surface had not consisted of these types of facets, as (111) specular scattering was still the most dominant feature. We therefore suggest that most of the step edges observed in this experiment are localized to small regions, arguably associated with small "micropits" arising from individual Ne^+-bombardment events[21] or from the coagulation of mobile defect species such as adatoms or vacancies.

V. CONCLUSIONS

This work was centered on the interpretation of fine structure observable in diffuse-intensity oscillations scattered from step edges. To date, no diffraction technique (other than HAS) has been able to measure intensity scattered only from step edges. Also, the interpretation of such data from any other diffraction method will not be as straightforward, as only the longer-range interaction potential of HAS can guarantee the negligible scattering factors from one type of step edge (e.g., down or up) in either positive or negative parallel momentum transfers.

A study of the step-edge-related structure factors for a model 1D stepped surface indicates that different types of interstep correlations can be identified. The calculations are then compared with experimental data from the Cu(111) surface. The exposure of lower-lying layers and the 3D lattice-gas-like nature of the extended step edges allows an absolute determination of the fcc crystal orientation. Elastic intensities from a defect-free fcc (111) face cannot be used to distinguish $\langle 11\bar{2}\rangle$ and $\langle \bar{1}\bar{1}2\rangle$ directions. Previously only the inelastic scattering from surface phonons was known to reflect the 3D nature of the substrate.[22]

A further comparison of the data with computations reveals that the ion-bombarded surface, as studied here, exhibits steps that are not randomly directed but that do have strong preferences to be oriented as the neighboring step edges—that is, microfacets have been formed which are of high step density. The presence of (331) and (211) microfacets has been implied. Whether the clustering of step edges arises after annealing processes, reflecting the dynamics of step-edge defects, or whether the microfacets arise directly from the sputtering process, remains a point of debate.

The 1D model of the surface assumes infinitely extended step edges. An equivalent 2D model should, in principle, allow broadening out of the scattering plane. We anticipate two distinct causes for out-of-plane broadening. The first arises from the presence of kinks along any individual step edge. The second arises from a lack of correlation in kink positions between pairs of independent step edges. These aspects of out-of-plane broadening have been thoroughly studied and simulated for the vicinal surfaces that undergo roughening.[23] This type of study would carry over to our case of microfacets, or for $P_{ch}\sim 0$. As far as we know, no theoretical studies of structure factors for step-edge scattering have been made for 2D systems with randomly oriented steps or for any cases where $P_{ch}\neq 0$ and $P_{ch}\neq 1$. For helium-scattering studies this is of utmost importance since, for most metallic surfaces, the large-angle diffusely scattered intensities arise almost wholly from step-edge diffraction. Terrace diffraction is centered very closely to the specular from the terraces only and, in any other direction, it is the step-up–to–step-up correlation (or the step-down–to–step-down correlation) that is of importance. This type of correlation is *not* equivalent to terrace-terrace correlations, which dominate diffraction peak shapes in (LEED),[5,24,25] or, indeed, specular scattering of HAS.

We have shown that the study of diffuse HAS intensities from monatomic step edges can yield not only information on local step-edge shapes, but also on the order along step edges and the interstep correlations. This type of information is not directly available from any other diffraction technique. We feel that studies of this type

will prove complementary to the very-well-developed high-resolution electron-diffraction methods for surface characterization. We hope also that measurements of this type will resolve the size of defect craters from individual bombardment events and/or the migration and coagulation of complex defect structures.

ACKNOWLEDGMENTS

We wish to thank G. Zhang and C. Koziol for allowing short interruptions of a measurement program and for the general running and upkeep of the experimental apparatus.

---

*Present address: AT&T Bell Laboratories, 600 Mountain Avenue, Murray Hill, NJ 07974-2070.

[1]G. C. Wang and T.-M. Lu, Surf. Sci. **122**, L635 (1982).

[2]K. D. Rendulic, A. Winkler, and H. P. Steinrück, Surf. Sci. **185**, 469 (1987).

[3]J. A. Serri, J. C. Tully, and M. J. Cardillo, J. Chem. Phys. **79**, 1530 (1983).

[4]See also, for example, G. A. Somorjai, *Chemistry in Two Dimensions: Surfaces* (Cornell University Press, Ithaca, NY, 1981).

[5]M. Henzler, Appl. Surf. Sci. **11/12**, 450 (1982).

[6]T. -M. Lu and M. G. Lagally, Surf. Sci. **120**, 47 (1982).

[7]L. K. Verheij, B. Poelsema, and G. Comsa, Surf. Sci. **162**, 858 (1985).

[8]A. M. Lahee, J. R. Manson, J. P. Toennies, and Ch. Wöll, Phys. Rev. Lett. **57**, 471 (1986).

[9]G. Drolshagen and R. Vollmer, J. Chem. Phys. **87**, 4948 (1987).

[10]B. J. Hinch, Phys. Rev. B **38**, 5260 (1987).

[11]B. J. Hinch, Surf. Sci. **221**, 346 (1989).

[12]B. J. Hinch, A. Lock, J. P. Toennies, and G. Zhang, J. Vac. Sci. Technol. B **7**, 1260 (1989).

[13]R. Berndt, B. J. Hinch, J. P. Toennies, and Ch. Wöll, J. Chem. Phys. **92**, 1435 (1990).

[14]C. Skorupka, Ph.D. thesis, Clemson University, 1989; J. R. Manson (private communication).

[15]G. Comsa, in *Dynamics of Gas Surface Interaction,* Vol. 21 of *Springer Series in Chemical Physics,* edited by G. Benedek and U. Valbusa (Springer, Berlin, 1981).

[16]J. P. Toennies, J. Vac. Sci. Technol. A **5**, 440 (1987).

[17]Ch. Wöll (private communication).

[18]A strong asymmetry in scattered intensity has been observed from Al(332). See, for example, B. J. Hinch, A. Lock, H. H. Madden, J. P. Toennies, and G. Witte, Phys. Rev. B (to be published).

[19]F. Fabre, B. Salanon, and J. Lapujoulade, Solid State Commun. **64**, 1125 (1987).

[20]G. Blatter and T. M. Rice, Phys. Rev. B **27**, 7051 (1983).

[21]This is contrary to the idea that a single ion produces a monovacancy. See, for example, B. Poelsema, K. Lenz, L. S. Brown, L. K. Verheij, and G. Comsa, Surf. Sci. **162**, 1011 (1985).

[22]V. Bortolani, A. Franchini, G. Santoro, J. P. Toennies, Ch. Wöll, and G. Zhang, Phys. Rev. B **40**, 3524 (1989).

[23]J. Villain, D. R. Grempel, and J. Lapujoulade, J. Phys. F **15**, 809 (1985).

[24]J. E. Houston and R. L. Park, Surf. Sci. **26**, 269 (1971).

[25]W. Aldhart, Acta Crytallogr. Sect. A **37**, 794 (1981).